The Iranian Journal of Mechanical Engineering Transactions of ISME
Journal homepage: https://jmee.isme.ir/
Vol. 24, No. 2, 2023, pp. 81-103

Research Paper

DOI: https://doi.org/10.30506/jmee.2023.2006028.1316

Bevel Pipe Inspection by Snake Robot

Alireza Javanbakht*
M.Sc. Student

Majid Sadedel†
Assistant Professor

Investigation on snake robots for pipe inspection purposes has been the subject of various papers. In this paper, we explore a unique type of snake robot that utilizes spherical modules. Ensuring proper contact between the robot and the pipe walls is crucial for successful climbing. If the normal force is too low, the friction force will not be enough for the robot to ascend, while excessive normal force can increase energy consumption. Therefore, it's necessary to investigate the robot's ability to move on sloped surfaces to ensure its practicality. In this paper, we present a new method for adjusting the robot's behavior on different surface slopes, which has been instrumental in optimizing its locomotion on sloped surfaces. Additionally, we have tested a novel torque control method to avoid boundary condition violations with promising results. The results of simulations conducted in MATLAB and Simulink have been validated by comparing them to existing experimental data. The simulations indicate that an excessive value of parameters in the proposed method can increase the generated torque by up to 295%.

Keywords: Mobile robots, Pipe inspection, Snake robots, Torque control

1 Introduction

1.1 Early developments, properties and potentials of snake robots

The original design of a snake-like robot dates back to the (1970s) when Professor Shigeo Hirose first introduced this idea. The concept of snake robots is inspired by the exceptional flexibility of snakes in nature. It is snake robots' kinematic redundancy that allows these robots to move in various ways. The high degree of freedom makes snake robots highly adaptable to different environments and enables them to accommodate themselves to their surroundings. The high degree of freedom in snake robots enables a diverse range of design possibilities and allows them to move in a variety of ways.

---

*M.Sc., Student, Tarbiat Modares University, Department of Mechanical Engineering, Tehran, Iran, alireza_javanbakht@modares.ac.ir
†Corresponding Author, Assistant Professor, Tarbiat Modares University, Department of Mechanical Engineering, Tehran, Iran, majid.sadedel@modares.ac.ir

Received: 2023/07/01, Revised: 2023/08/28, Accepted: 2023/12/27

This feature also makes it possible for snake robots to navigate through narrow channels and pipes, traverse rough or flat surfaces, pass by or climb over obstacles obstructing their path, and even climb vertical pipes from inside or outside [1]. Also, the features of snake robots enable them to swim and travel in water [2]. The versatility of snake robots makes them ideal for a wide range of applications, including search and rescue, inspection, and maintenance in various industrial settings.

1.2 Different kinds of snake robots and their locomotion

1.2.1 Snake robots with wheels

There are some researches in which snake robots are designed with active wheels [3],[4],[5]. In a research work in (2009) which has been done by Fjerdingen et al. [3], the designed robot has active wheels which can help the robot climb a vertical pipe from inside. To begin its movement, the snake robot first establishes contact with the pipe wall at a minimum of three points. Once this contact is made, the active wheels begin rotating, and the robot moves in the desired direction inside the pipe. In some research works in (2016), (2018) and (2020), [6],[7],[8], snake robots are designed with passive wheels, which are called non-holonomic snake robots.

1.2.2 Snake robots without wheels

Not all snake robots are designed with either active or passive wheels. Some robots employ alternative methods of locomotion. For example, in a research work by Chen et al. [9] in (2007), a traveling wave method is used to facilitate robot movement. In some research works which has been done in (2015) and (2020), [10],[11], robot joints are translational and rotational. In this kind, both rotational and translational actuated joints are involved in robot locomotion. Another study conducted by Javaheri Koopaee et al. in (2019) [12], a pedal wave method is employed, which mimics the movement of snails. Another locomotion method that has been used in some other research works in (2019) and (2020) [11],[13], is that robot moves by constricting and straightening its body (like a concertina). This method is called concertina locomotion. In some other research works in (2020) and (2021), snake robot locomotion via traveling wave has been investigated[14],[15].

1.3 Robot movements inside a channel or a pipe

Over time, several types of robots have been developed for inspecting channels and pipelines. For instance, Kim et al. [16] proposed a mechanism for the MRINSPECT VI (Multifunctional Robotic crawler for In-pipe inspection VI) in-pipe robot that is used for gas pipeline inspection. The robot has both active and passive wheels on three sides, which allows it to stick to the pipe walls and move in the desired direction.

Snake robots have garnered significant attention in the pipeline and inaccessible places inspection fields due to their unique properties.

In (2003), Wakimoto et al. [17] designed a snake robot specifically for inspecting pipes with diameters ranging from 18 to 100 millimeters. This robot moves inside a pipe via a traveling wave.

In (2010), Shin et al. [18] have developed a snake robot with the capability to climb vertical pipes. A combination of holding and sinusoidal motions was utilized in this design. While some modules maintain the robot's position by pushing its body against the walls to induce friction, other modules move the robot in the desired direction. These modules change their roll, resulting in the robot's ascending the vertical pipe.

In (2018), Whitman et al. [19] conducted research on using a snake robot for inspecting inaccessible places. In a notable example, the snake robot was deployed to assess a damaged building following the (2017) earthquake, demonstrating the robot's versatility in real-world scenarios.
Virgala et al. [15],[20] have developed a unique wheelless snake robot specifically designed for inspecting the inside of channels and pipes. The robot's motion is propelled by the friction between the channel walls and its body. The locomotion of this robot has been studied in both straight and curved pipes using a trapezium-like traveling wave. However, its locomotion on bevel surfaces has not yet been investigated. Due to pipe inspection challenges, practicability of this robot cannot be guaranteed unless its motion on sloped surfaces is investigated.
This paper investigates a new method for adjusting the behavior of the wheelless snake robot consisting of multiple modules [15],[20], to changes with the slope of the pipe. The proposed method involves altering the trajectory planning according to the slope of the surface where the robot is moving. Additionally, the method enables the control of the actuators to produce torque proportional to the surface slope. This innovative approach has the potential to enhance the robot's performance in navigating sloped surfaces. Furthermore, a new method to avoid violation of geometric boundary conditions for locomotion of this robot in pipes and channels is presented in section (2.1).
In the first chapter, we offer a comprehensive overview of the development of snake robots and summarize previous research works in the field. Moving on to chapter (2), we present the structure and locomotion of the robot, providing detailed explanations. Chapter (3) focuses on simulation, where we explore various aspects and provide in-depth explanations. In chapter (4), we present the verification process and share the obtained results. Finally, the last chapter concludes the study and proposes future research directions.

2 Robot structure and locomotion

In this study, we focused on the development of a unique wheelless robot designed to navigate through pipes and channels. The robot's movement is achieved through friction between its body and the walls of the pipe or channel. Previous research by Virgala et al. [15] served as inspiration for this project. The robot is composed of links connected by revolute joints and spherical components that are centered by revolute joints with a radius equivalent to half of the links' length. As can be observed in Figure (1), the robot looks like a group of spheres connected to each other.
Channel diameter is illustrated by D, and length of every link is presented by L; according to Figure (1(a)):

$$d = D - L \tag{1}$$

This robot utilizes a trapezoidal traveling wave for locomotion. The angle between the robot's body and the channel wall, as shown in Figure (1), is denoted by α.

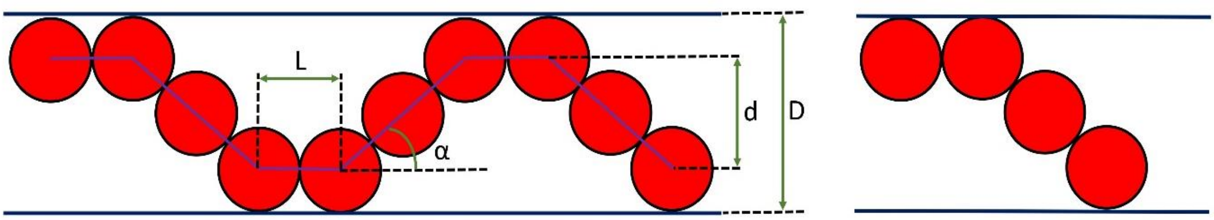

Figure 1(a) Snake robots' structure and some defined variables, **(b)** Amplitude links shape

The "Number of amplitude links," denoted as n_A, refers to the number of modules, each representing a spherical part of the robot, that can form a shape similar to Figure (1(b)).
It is evident that the value of n_A is dependent on D, L, and α. It is crucial to adjust n_A in such a way that α remains within an appropriate range. In previous research works [15], n_A was evaluated manually. However, in this study, a formula is introduced to calculate n_A while ensuring that α remains close to π/4:

$$nA = \mathrm{Ceil}\,\left(\frac{d}{(\sin(\frac{\pi}{4})\times L)} + 2\right) \tag{2}$$

In Equation (2), the "Ceil" function rounds the value to lower integer.
Once n_A is calculated, α can be computed. However, it is important to note that soft contact between the robot and the channel does not guarantee locomotion without slipping. To address this, a small value is added to the channel diameter. This allows trajectory planning to be conducted under the assumption of a penetration between the robot and the channel wall, which in turn increases the friction force. The extent of this penetration can be adjusted by setting a value for Dpenetration.

$$\alpha = \sin\text{-}1\,\frac{(D + \mathrm{Dpenetration} - L)}{(L\times(n_A - 2))} \tag{3}$$

The trajectory planning result is presented in the form of a matrix, which shows the angle of each joint at the end of each step within a single locomotion cycle.
The number of steps in a locomotion cycle, represented by the number of rows in the motion matrix, can be calculated using the following equation. As can be observed, it is solely dependent on the number of amplitude links.

$$P = 2\,(nA - 1) \tag{4}$$

The number of columns in the motion matrix corresponds to the degree of freedom of the robot and can be computed using the following formula. N represents the number of links of the robot.

$$DOF = N - 1 \tag{5}$$

Figure (2) illustrates the various stages of the robot's motion. In the second stage, the robot assumes an initial shape. Subsequently, the robot initiates its motion and successfully completes one motion cycle consisting of 6 steps (in this particular case, the number of steps in one locomotion cycle is 6). In the eighth stage, the robot repeats its motion cycle and returns to the second stage form. According to the Figure (2) matrix of motion is:

$$M = \alpha \begin{bmatrix} -1 & 0 & 1 & 1 & 0 & -1 & -1 & \dots \\ -1 & -1 & 0 & 1 & 1 & 0 & -1 & \dots \\ 0 & -1 & -1 & 0 & 1 & 1 & 0 & \dots \\ 1 & 0 & -1 & -1 & 0 & 1 & 1 & \dots \\ 1 & 1 & 0 & -1 & -1 & 0 & 1 & \dots \\ 0 & 1 & 1 & 0 & -1 & -1 & 0 & \dots \\ \dots & \dots & \dots & \dots & \dots & \dots & \dots & \dots \end{bmatrix} \tag{6}$$

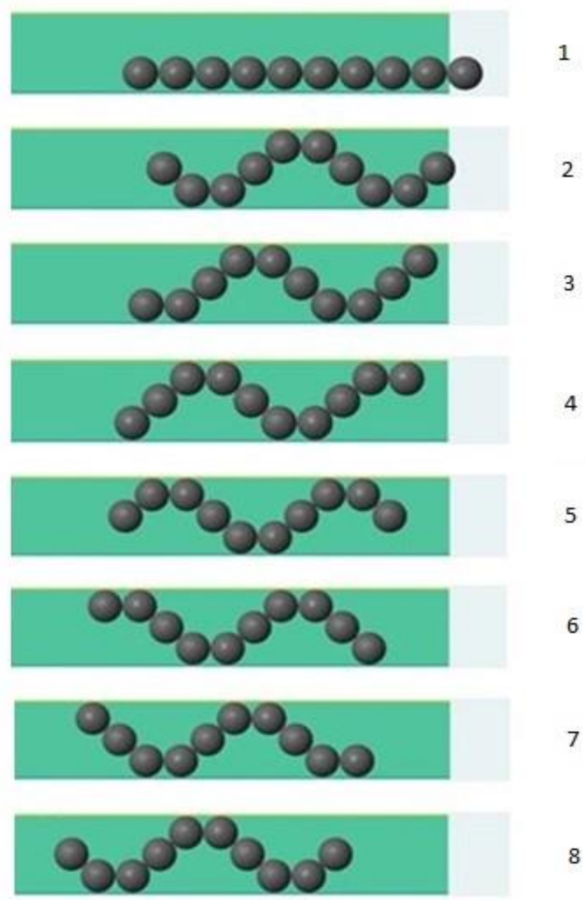

Figure 2 Getting into initial form and a six-phase locomotion cycle

Using matrix M, the angle of each joint of the robot at any step of motion can be calculated using the following equation:

$$qi(M) = Mr\text{-}1,i + Fr,i(f\,dir)\ k\ |\ Mr,i - Mr\text{-}1,i\ | \tag{7}$$

In Equation (7), Let $M_{r-1,i}$ represent the angle of the i-th joint in the r-1-th step. Additionally, k is a variable that ranges from 0 to 1. $F_{r,i}$ denotes a value from matrix F, which is responsible for adjusting the direction of motion. This value is computed using the following equation.

$$F = \begin{cases} \text{If } r = 1 & : \quad \text{Sign}\,(M_{r,i} - M_{r+p-1,i}) \\ \text{Else} & : \quad \text{Sign}\,(M_{r,i} - M_{r-1,i}) \end{cases} \tag{8}$$

In Equation (8), the “Sign” function gives -1 for negative values and +1 for positive values.
The locomotion method employed by this robot involves the utilization of propagating trapezoidal traveling waves. In order to achieve this specific type of motion, a time delay must be incorporated between the movements of each pair of adjacent joints. The front joints initiate their movement earlier, causing the wave to commence at the front section of the robot and propagate towards the modules located at the rear. The following equation demonstrates this fact:

$$t(M_{r,i+1})) = t(M_{r,i}) + \Delta t \tag{9}$$

So the time difference between the first joint and the last joint is:

$$t(M\,r, N-1) = t(Mr, 1) + (N-1)\Delta t \tag{10}$$

In this study, movement is achieved through the utilization of torque control, which differs from previous research efforts. The torque applied to each joint is determined by the disparity between the desired trajectory and the actual value, which is gathered by sensors.
Angular difference, angular velocity difference, and angular acceleration difference are used to calculate applied torque:

$$\tau = Ae + B\left(\frac{de}{dt}\right) + C\left(\frac{d^2e}{dt^2}\right) \tag{11}$$

A, B and C are coefficients that depend on physical properties.
To enable continuous motion of the robot, two functions have been defined. The first function is responsible for adjusting the step of motion for each joint at any given moment during the motion:

$$r=1 + \mathrm{Floor}\left(\frac{(t - fixtime - (\Delta t \times i))}{(t_{onemove} + \Delta t)}\right) - \left(p \times \mathrm{Floor}\left(\frac{(t - fixtime - (\Delta t \times i))}{((t_{onemove} + \Delta t) \times p)}\right)\right) \tag{12}$$

In Equation (12), the “Floor” function rounds the value to lower integer.
The other function is $t_{operation}$. Due to the fact that the period of each move is $t_{onmove}+\Delta t$, $t_{operation}$ adjusts the amount of this time that has been passed for every joint in every step, so this parameter fluctuates between 0 and $t_{onmove}+\Delta t$.

$$\begin{aligned} toperation = t - fixtime - \big((t_{onemove}) \times (r-1) + (\Delta t \times i) \big) - \\ \left(p \times (t_{onemove} + \Delta t) \times \left(\mathrm{Floor}\left(\frac{t - fixtime}{(t_{onemove} + \Delta t) \times p}\right)\right)\right) \end{aligned} \tag{13}$$

2.1 The Necessity of not violating physical boundaries

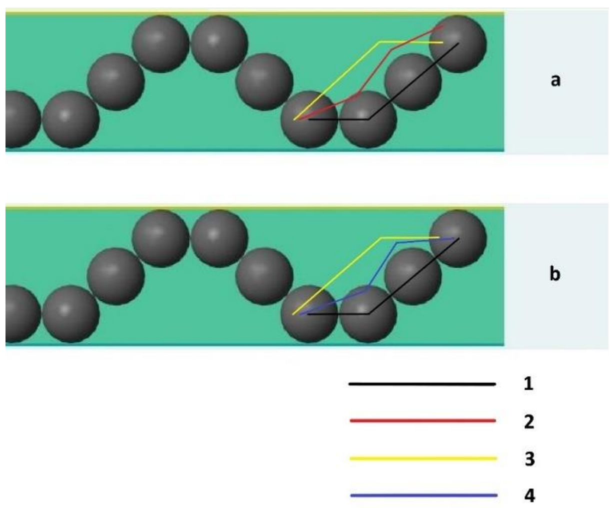

Figure 3 The necessity of not violating physical boundaries

When operating in confined spaces, one of the primary challenges for robotic locomotion is the avoidance of physical barriers. To ensure unrestricted movement, the robot must meticulously plan its motion while respecting physical boundaries. This necessitates a specialized approach to motion planning that considers factors such as the robot's size, shape, and the surrounding environment. By skillfully maneuvering around obstacles and maintaining a safe distance from walls and other barriers, the robot can achieve smooth and efficient movement in restricted spaces. To provide a visual representation of this issue, let's consider the scenario depicted in Figure (3). The upper panel of the figure displays the robot's position at various moments during a movement phase. Each color in the figure represents the robot's position at a specific point in time. Suppose the robot starts its motion from position (1) and moves in the order (1-2-3). In this case, several problems arise; as shown in Figure (3), the robot cannot reach position (2) without violating the physical boundaries, since it is beyond the channel walls. So, according to Figure (3(a)), the robot should make its motion in another way; in this case, the robot should go to position (4) after position (1).

Previous research has commonly applied the potential fields method to incorporate boundary conditions into robotic motion planning. However, in this study, a different approach is adopted, where the robot's control system is based on torque control. Specifically, a saturation torque is set to limit the maximum torque produced by any actuator. By incorporating the saturation method into the robot's control system, the robot can effectively harmonize its motion with the boundary conditions. This approach prevents the robot from generating excessive torque to reach an unattainable position, thereby ensuring that the robot moves within the specified limits. In other words, the torque control system enables the robot to correct any errors in trajectory planning, even if the planned trajectory does not take boundary conditions into account.

In this research, trajectory planning has been done in MATLAB, and the robot's motion in a channel with a rectangular cross-section has been tested and analyzed in Simulink.

Trajectory planning calculations can be summarized in Figure (4).

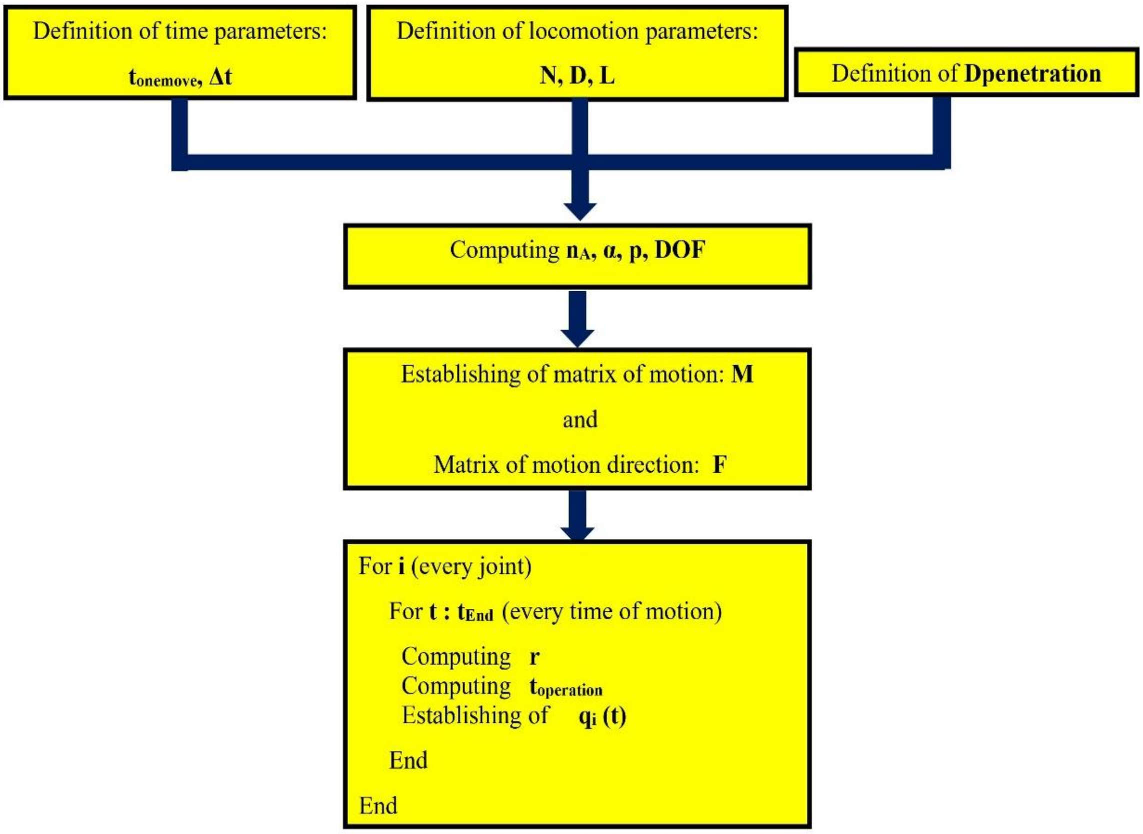

Figure 4 Trajectory planning procedure flow chart

2.2 Robot locomotion a sloped channel

The snake robot primarily relies on friction with the channel side walls to move. While friction is the only force that needs to be considered for locomotion on a flat surface, on sloped channels the force of gravity is brought into consideration, which can conflict with the robot's motion. To address this issue, the Dpenetration parameter, which was previously discussed in section (2), has been modified to analyze its impact on the robot's locomotion on beveled surfaces. Adjusting the Dpenetration parameter enables the robot to enhance the necessary friction force to overcome gravity, allowing it to move smoothly and efficiently on sloped surfaces. However, increasing this parameter affects the trajectory planning of the robot, as it must be aligned with the increased friction force with the surrounding walls. This increased parameter value also results in higher torque requirements for the robot's actuators; a great value for Dpenetration can saturate actuators.

In summary, it is crucial to select an optimal value for Dpenetration. This value should not only ensure sufficient friction force for the robot to climb a sloped canal but also be optimized to allow the robot to execute its motion with reasonable actuator torques.

To determine the appropriate value of Dpenetration for each slope, the robot's motion was tested with various values of this parameter across different slopes. The results were then analyzed to identify the appropriate function for calculating the optimal value of Dpenetration.

3 Modeling

This study focuses on the locomotion of a snake robot in a straight channel with a rectangular cross-section. Table (1) presents the properties of the robot, including the number of links, length of each link, channel diameter, friction coefficient between the robot and channel walls, and weight of each module.

Furthermore, Table (2) illustrates the time required for one move in each level of motion, the time delay, and the duration of time it takes for the robot to reach the initial position before starting the motion, which is referred to as "fixtime".

As mentioned previously, the "k" function determines the manner in which the angle changes in each step. The "k" function is defined as follows:

$$k=0.5\left(1-\cos\left(\frac{(\pi t_{operation})}{t_{onemove}}\right)\right) \quad (14)$$

The function for "k" is depicted in the plot below. It is evident that this function is highly suitable for angle change, as the values of angular velocity, angular acceleration, and angular jerk are reasonable, according to Figure (5).

Table 1 Physical properties value

Parameter	Value
N	11
L	0.105m
D	0.18m
μ_k	0.5
μ_s	0.7
w	0.406kg

Table 2 Time properties value

Parameter	Value
$t_{onemove}$	1.5(s)
Δt	0.01(s)
fixtime	1.5(s)

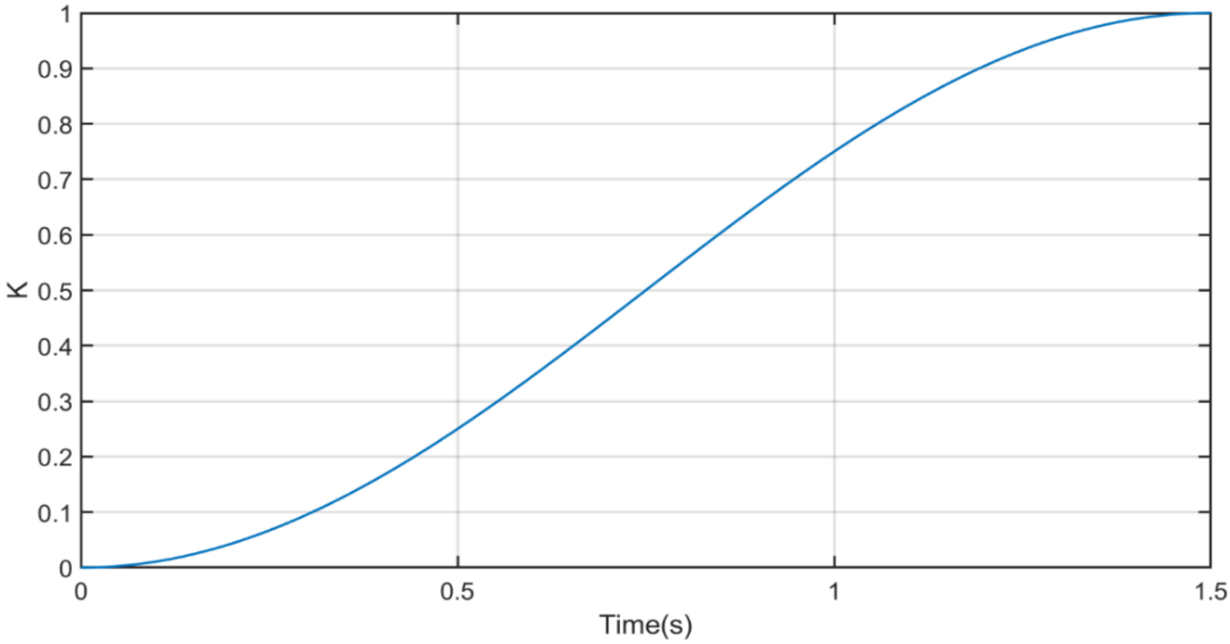

Figure 5 Value of "k" between 0 and 1.5 (if tonemove=1.5s)

4 Results

Given the use of alternative methods and equations in this paper, as well as the adoption of torque control, it is necessary to validate some of the results against prior research. To accomplish this, the head and rear joint angles during several locomotion cycles were compared to experimental results from previous research. This enables us to confirm the validity of our approach and assess its consistency with established findings [15].

Based on the results shown in Figure (6), the findings of this paper closely align with the research conducted by Virgala et al [15]. However, it is important to note that while the results of Virgala et al were obtained through experimentation, the results presented in this paper are based on simulations. Therefore, it is reasonable to expect some slight differences between these two sets of results.

In this section, the simulation results for the motion of the robot in a channel with a rectangular cross-section are presented and analyzed. The simulation covers a duration of 10 seconds, during which the robot's motion is observed and evaluated.

In Figure (7), the generated trajectory for each joint is shown. All joint angles start at zero. The robot then enters the initial phase, where it positions itself near the channel walls and prepares for motion. This phase typically lasts around 1.5 seconds. Subsequently, the robot initiates a trapezoidal traveling wave to commence its motion. Figure (7) illustrates the planned trajectory for three neighboring joints (joints (3), (4), and (5)). It is worth noting that, as per the motion matrix, there is a slight delay in trajectory planning for the two adjacent joints.

As was mentioned before, in this research, the robot's control system is based on torque control. The robot can synchronize its motion with boundary conditions by utilizing saturation, which prevents the robot from exerting excessive torque and reaching an unattainable position. Due to this saturation, there may be a discrepancy between the trajectory and the actual angles of each joint. This error arises because of the torque control mechanism that automatically corrects the motion when it conflicts with a physical boundary condition. Figure (8) shows the angular error between trajectory and results from simulation. It can be observed clearly from Figure (8) that peaks of error occur when there is a conflicting boundary condition, so not only is the value of error acceptable, but it is also essential for the robot's motion.

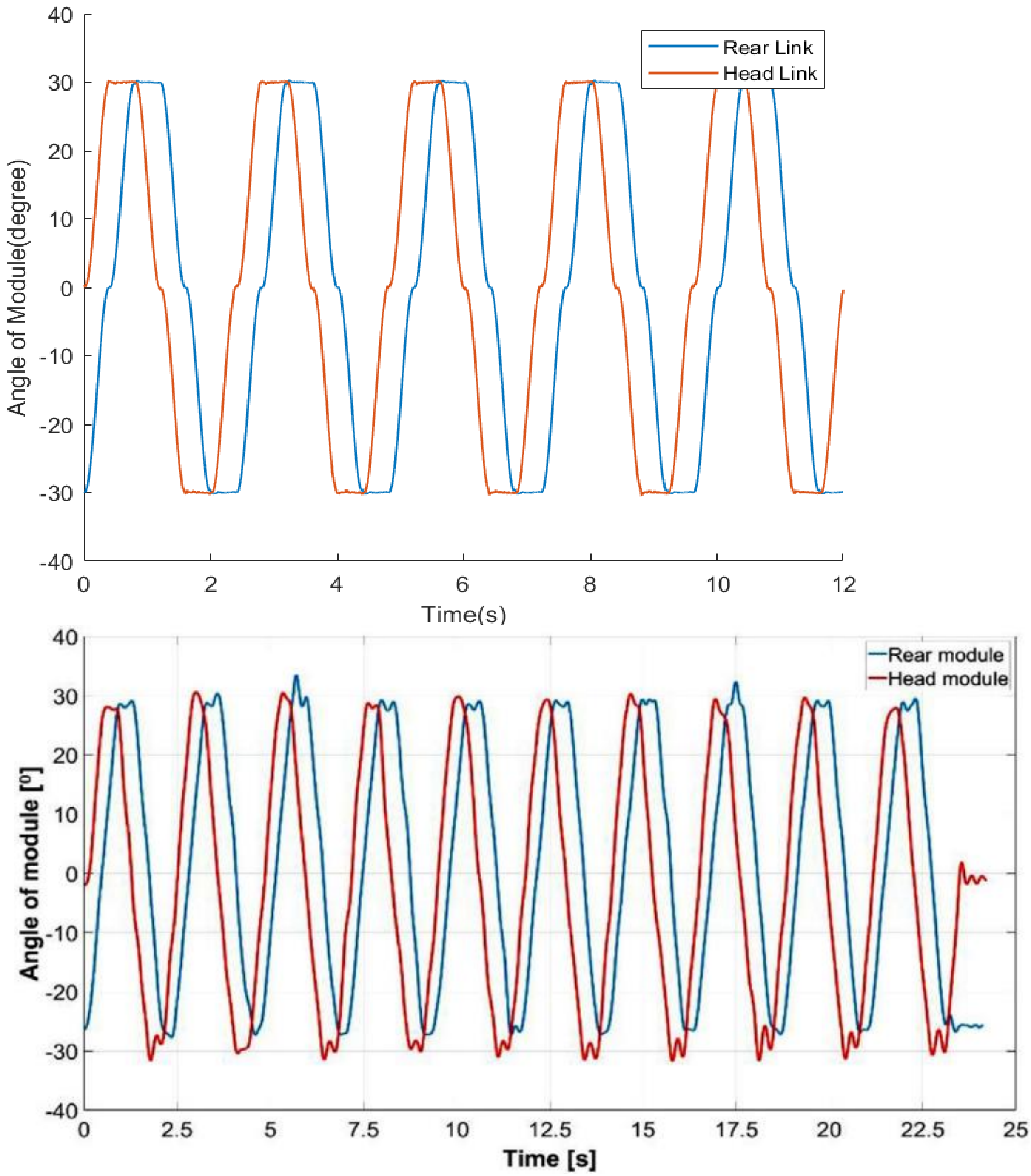

Figure 6 Top:Head and rear joints' angles from simulation in this research
Bottom: Head and rear joints' angles in Virgala et al research [15]

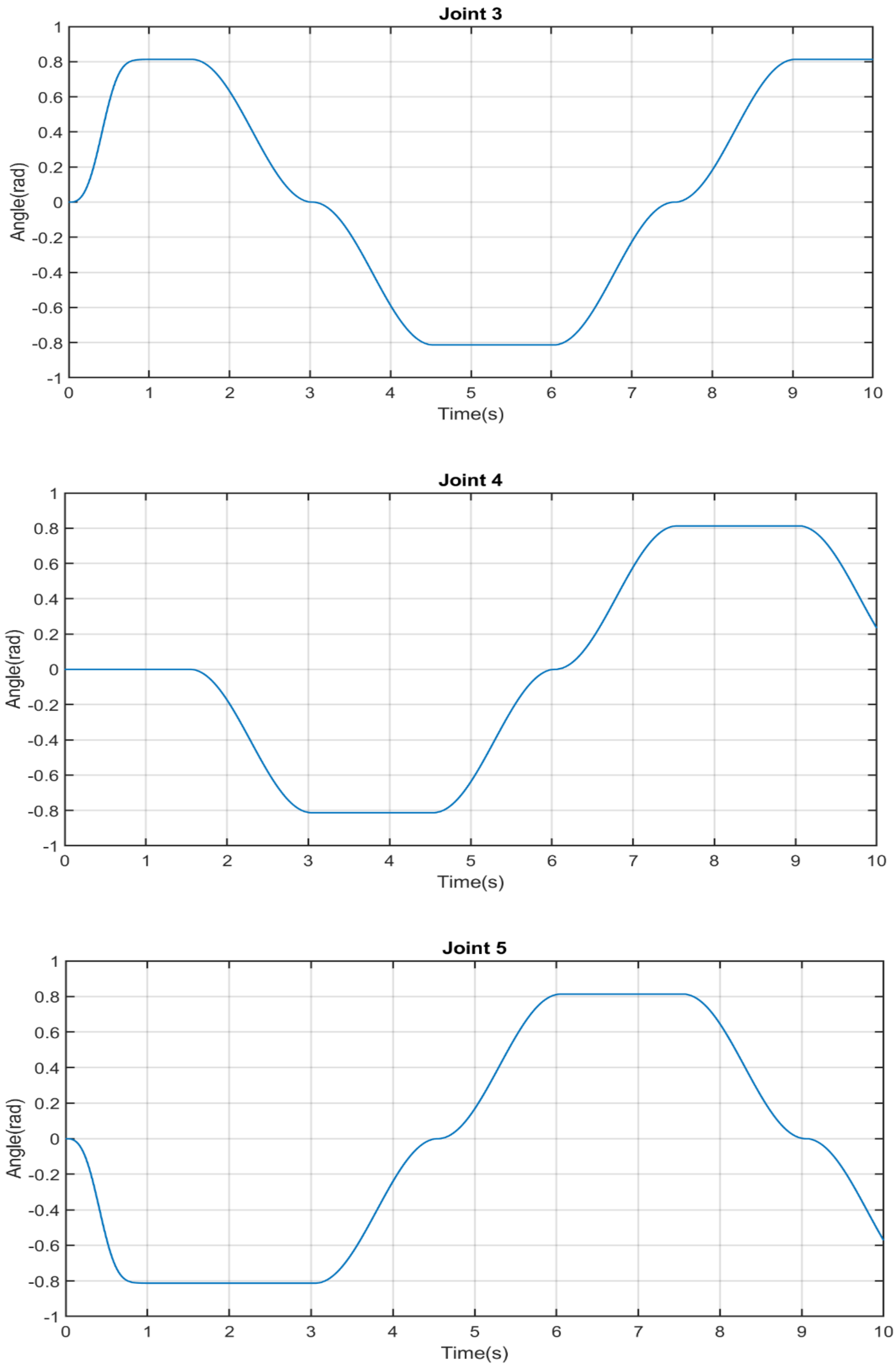

Figure 7 Planned trajectory for three joints with zero penetration for 10 seconds

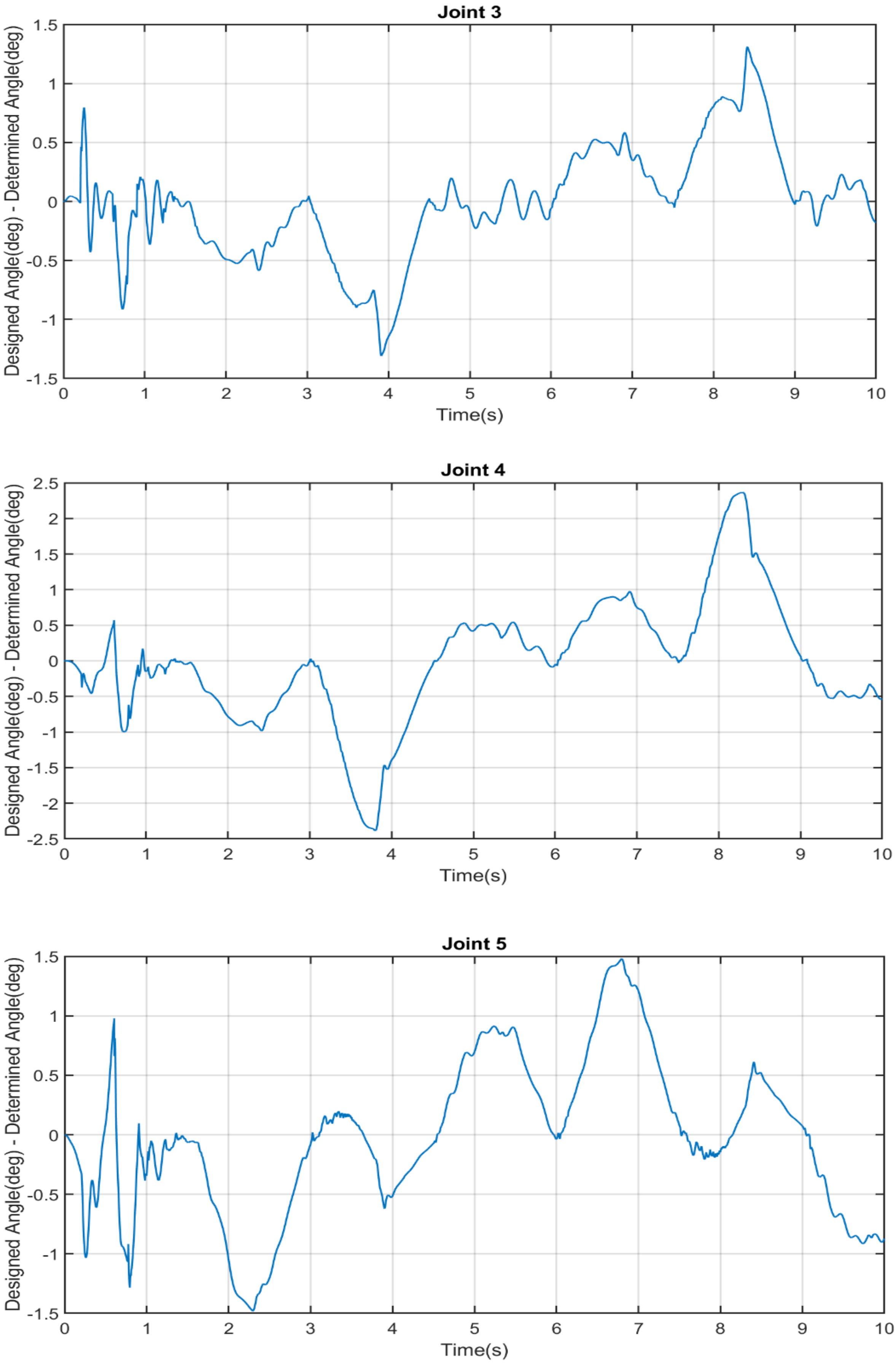

Figure 8 Angular error between trajectory and simulation results for three joints with zero penetration

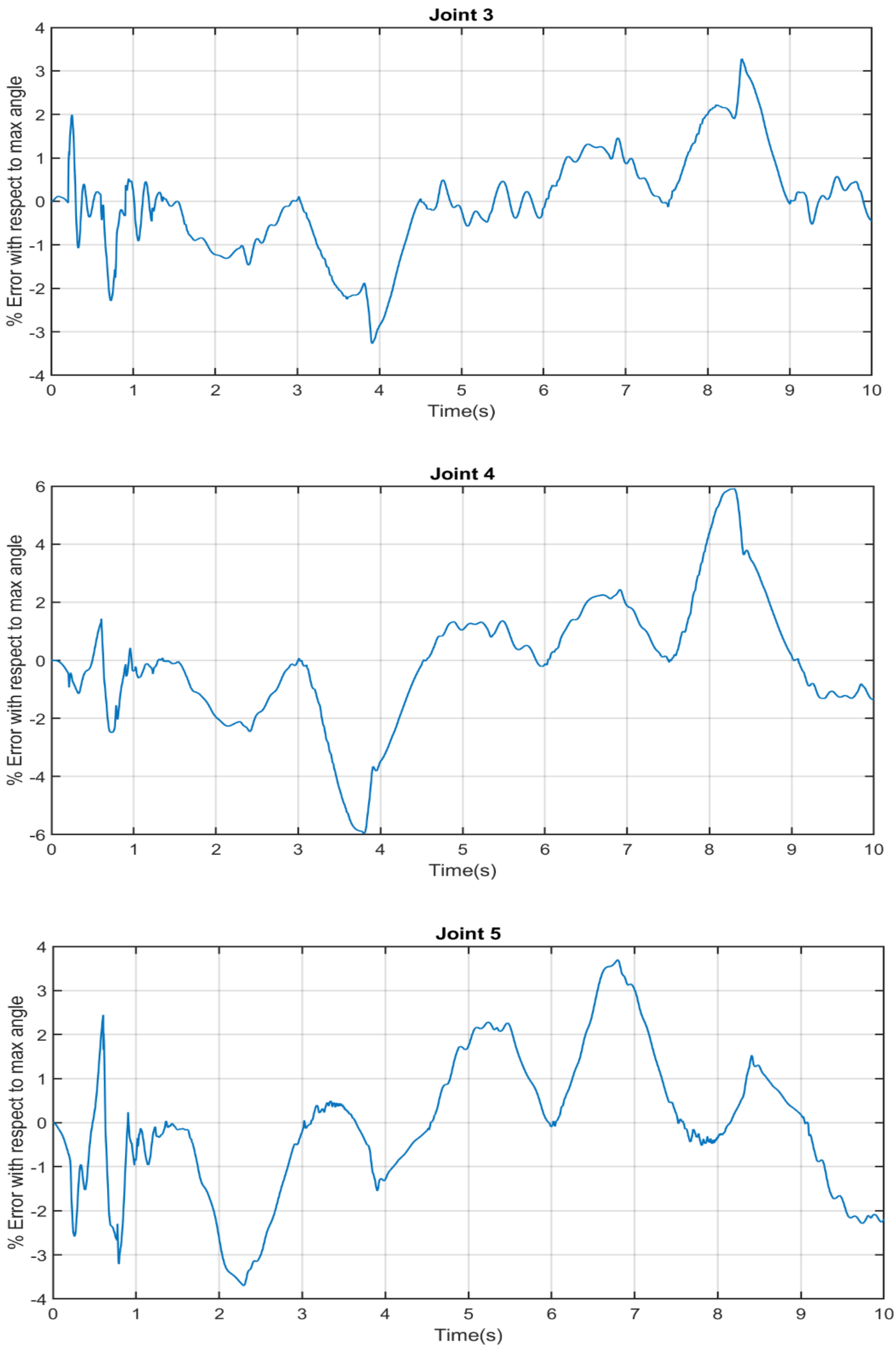

Figure 9 Percentage of angular error for three joints with respect to maximum designed angle in trajectory

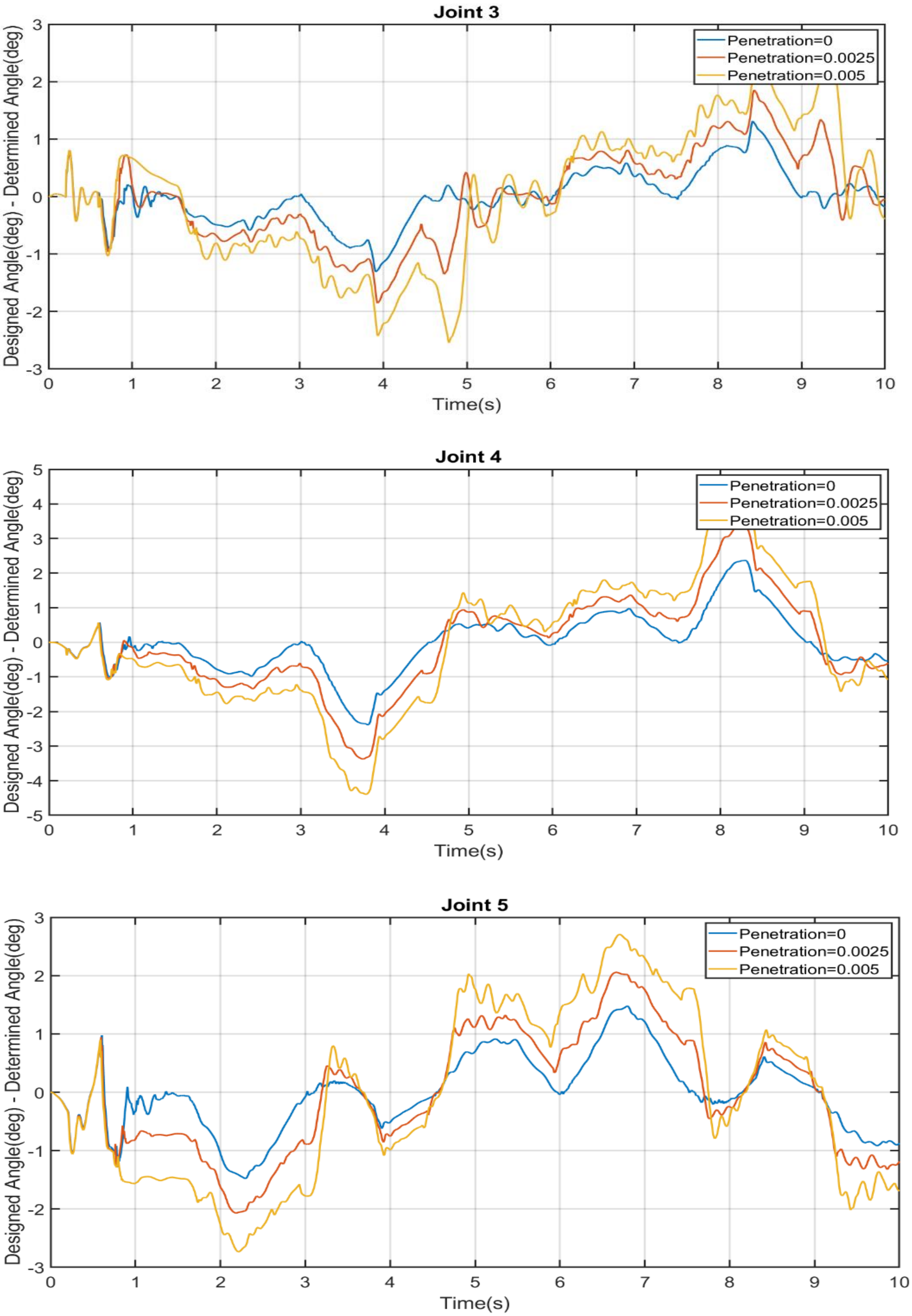

Figure 10 Angular error between trajectory and simulation results for three joints with zero penetration for three penetrations

It can be seen from Figure (11) that the rise of penetration can result in the rise of needed torque which can saturate actuators in some cases. The increase in error is correlated with the increase in generated torque. As mentioned in previous sections, the generated torque is calculated based on the error, its integration over time, and its time derivatives. Therefore, the change in generated torque is a direct consequence of the increase in error, which is caused by the increase in penetration.

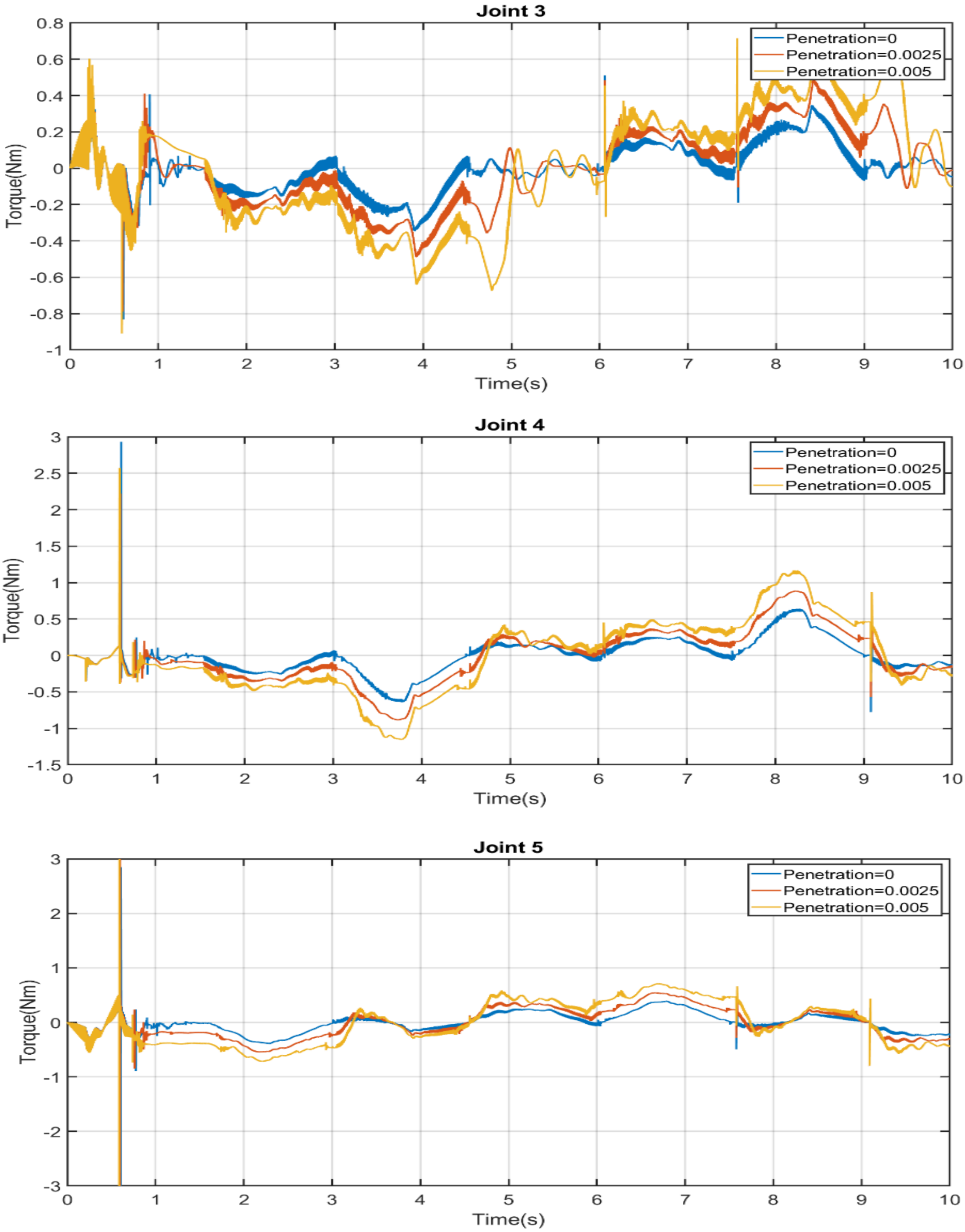

Figure 11 Generated torque for three joints for three penetrations

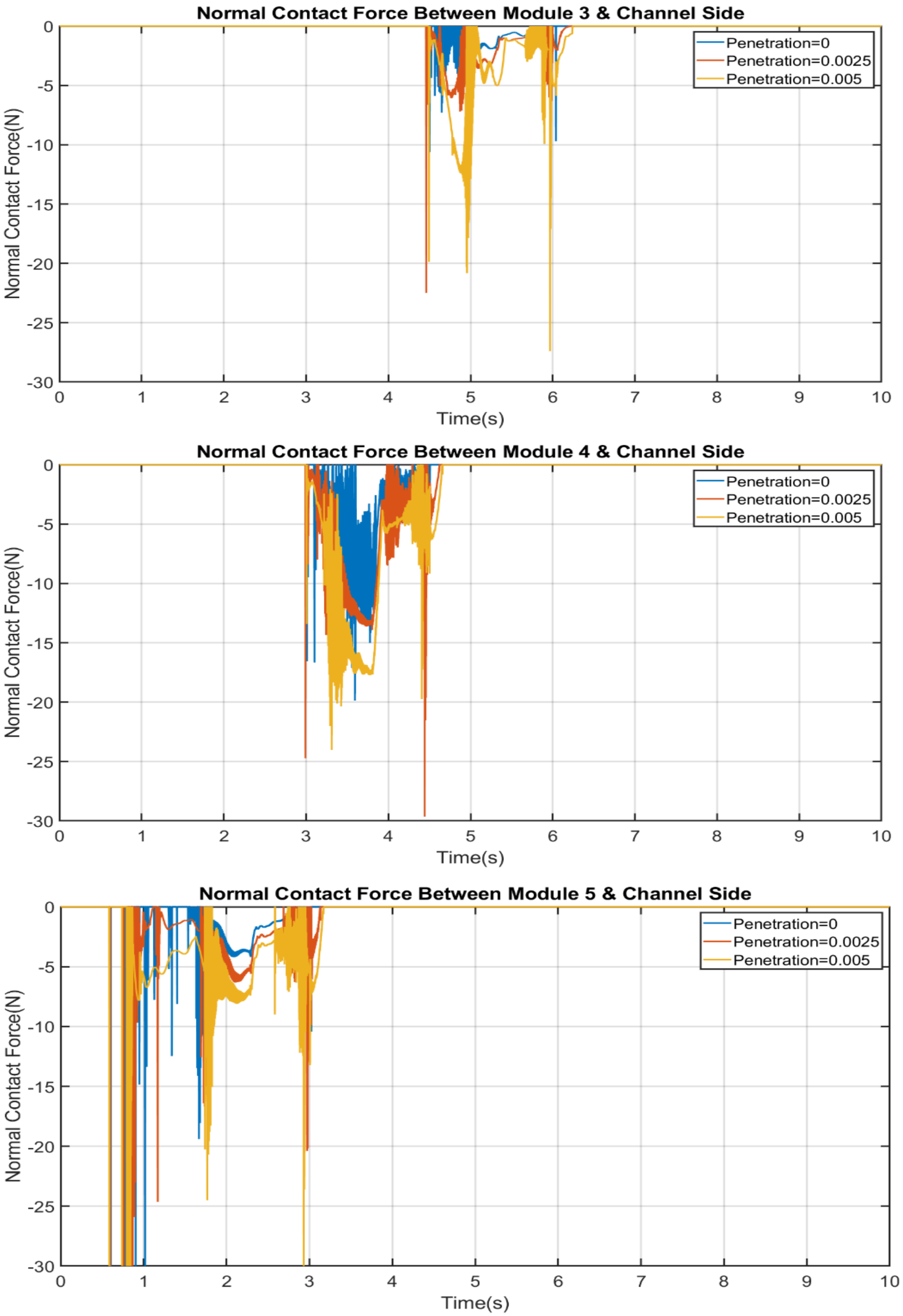

Figure 12 Normal contact force between one of the side channel walls and for three modules for three penetrations

For locomotion in bevel channels and pipes, a higher friction force is needed to conflict with the force which is caused by gravity. One way to increase friction force is by increasing normal force. In this robot, to increase normal force, one way is to increase penetration value; because according to Figure (11) rise of penetration value can make a higher error which can cause a higher value of generated torque. The higher torque pushes the snake robot's modules to channel walls and provides a higher normal force which can increase friction between the robot's modules and channel walls and make locomotion in a sloped channel possible.

In Figure (12), the normal force between one of the channel side walls and three of the robot's modules is illustrated. This graph proves the propounded theory about the effect of penetration and normal contact force. It can be seen that higher penetration value results in higher normal force that can provide higher friction that can stop robot from slipping on bevel surfaces.

As discussed previously, an increase in the penetration value can lead to actuator saturation. Therefore, it is crucial to determine an optimized value for penetration that provides sufficient friction without causing actuator saturation or locomotion issues. To achieve this, the traveled distance of the robot within a specific time is compared for different slopes and various penetration values. This analysis aims to identify the optimum penetration value for each slope angle. Figure (13) displays the robot traveled distance with respect to surface slope and penetration in the form of a 3D graph. According to the findings depicted in Figure (13), if the penetration value is inadequate, the robot may either fail to move up or the traveled distance will be insignificant.

Additionally, it is evident from Figure (15) that a higher slope angle necessitates a higher penetration value. Furthermore, based on the observations from Figure (13) and Figure (14), there is a decrease in the traveled distance between the section where the robot is unable to move and the section where it successfully moves forward. This decline occurs because the starting point for calculating the traveled distance is the position of the robot's last module at the end of the fixation time.

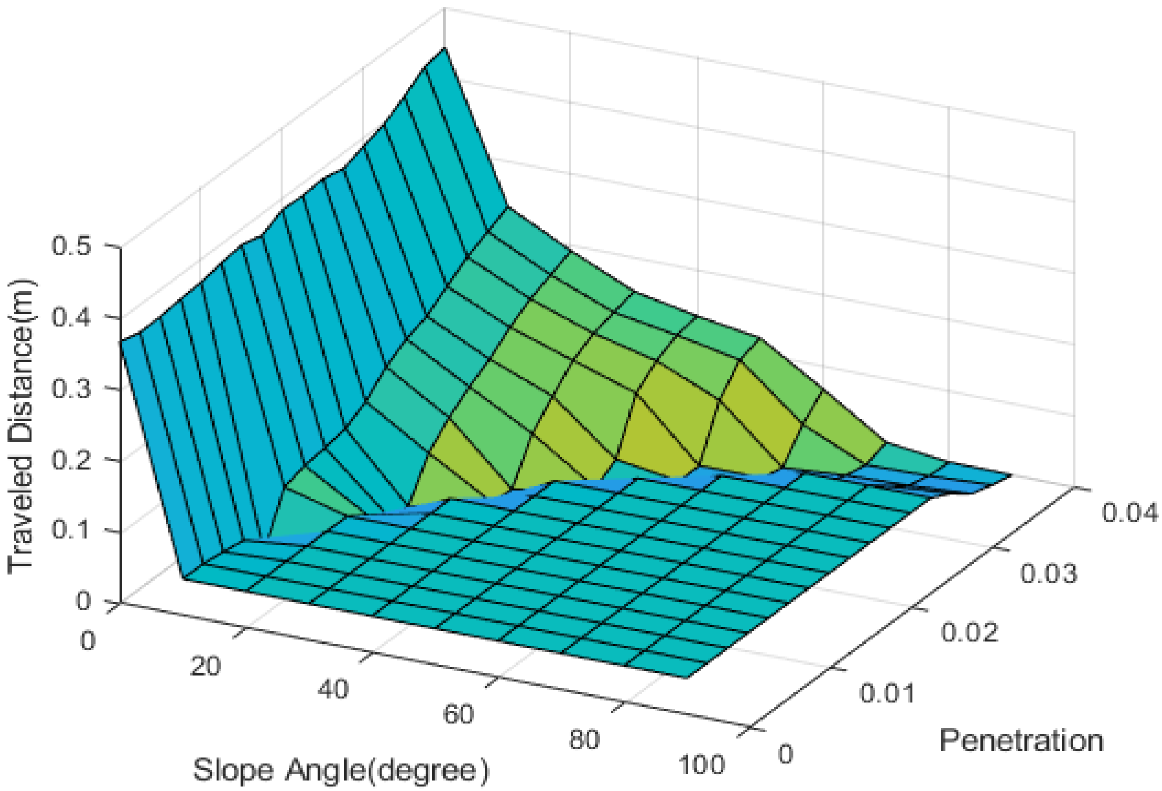

Figure (13) Traveled distance for different slopes and penetrations) (Slope Angle From 0^o to 90^o)

When the penetration reaches its critical value, the robot adheres to the channel walls in the initial state and does not slip. However, during other locomotion steps, the robot experiences slipping. In lower penetration values, even in the initial state, the robot slips, which results in a lower traveled distance. The part of the diagram between 0° and 20° is very important, so this part has been plotted more precisely in Figure (14) and Figure (16). It can be seen that all the above-mentioned descriptions are true about Figure (14) too. Also, Figure (16) demonstrates the effect of slope angle and penetration on traveled distance, more precisely between 0° and 20°.
It is worth mentioning that, as shown in Figure (17), a higher penetration value requires a higher input torque. For instance, at time=1s, the generated torque for Dpenetration=0.04m is 195% greater than the generated torque for Dpenetration=0.0325m. Additionally, the traveled distance for Dpenetration=0.04m is 26% higher than the traveled distance for Dpenetration=0.0325m at the same slope.
The proposed function for calculating $D_{penetration}$ is:

$$\mathrm{Dpenetration(optimized)} = (0.06\sin(\pi(\frac{\mathrm{Slope(degree)}}{180}))) + 0.02 \tag{15}$$

A function has been proposed to calculate the appropriate penetration value for each slope. Figure (18) illustrates the plot of this function. It is evident that this function connects the optimum points from Figure (13), considering the traveled distance. Additionally, the points on this function do not include excessive penetration values that would lead to an unnecessary increase in required torque.

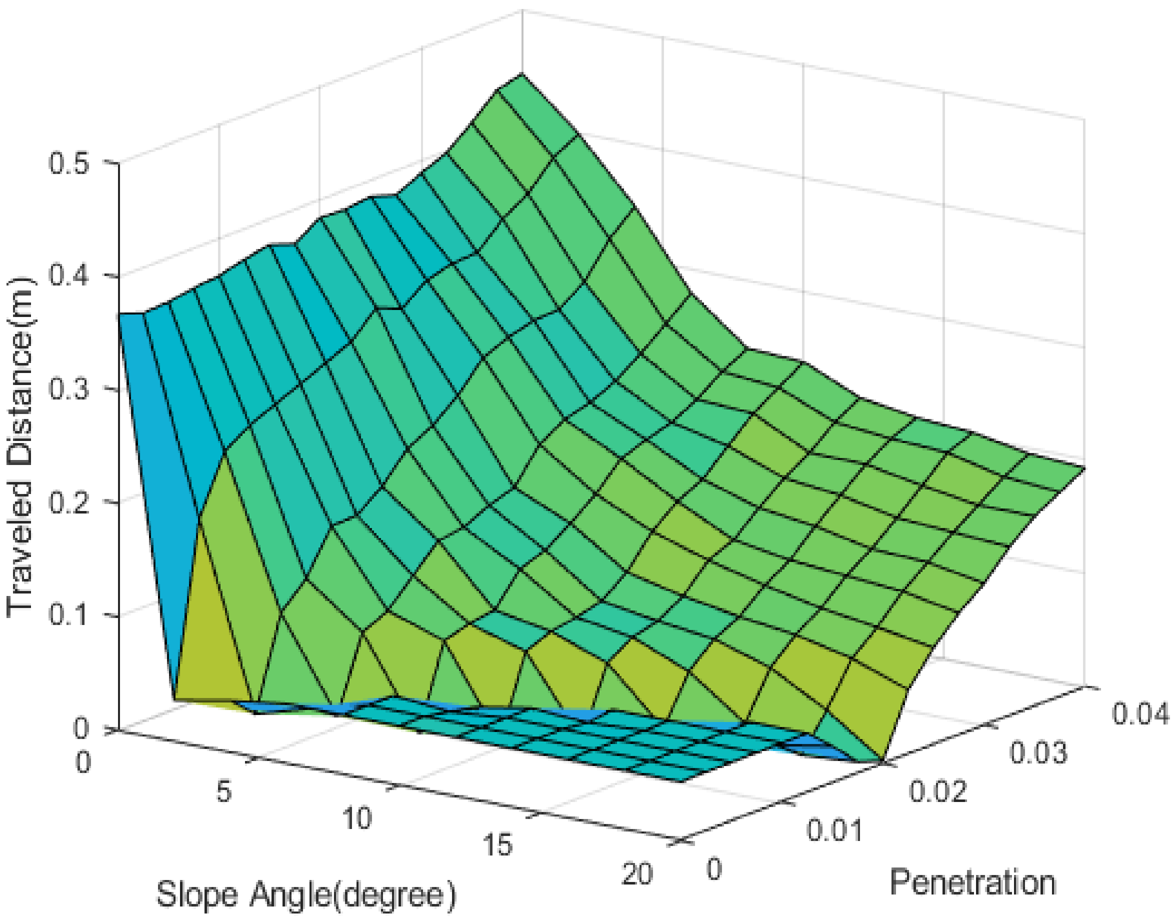

Figure 14 Traveled distance for different slopes and penetrations) (Slope Angle From 0° to 20°)

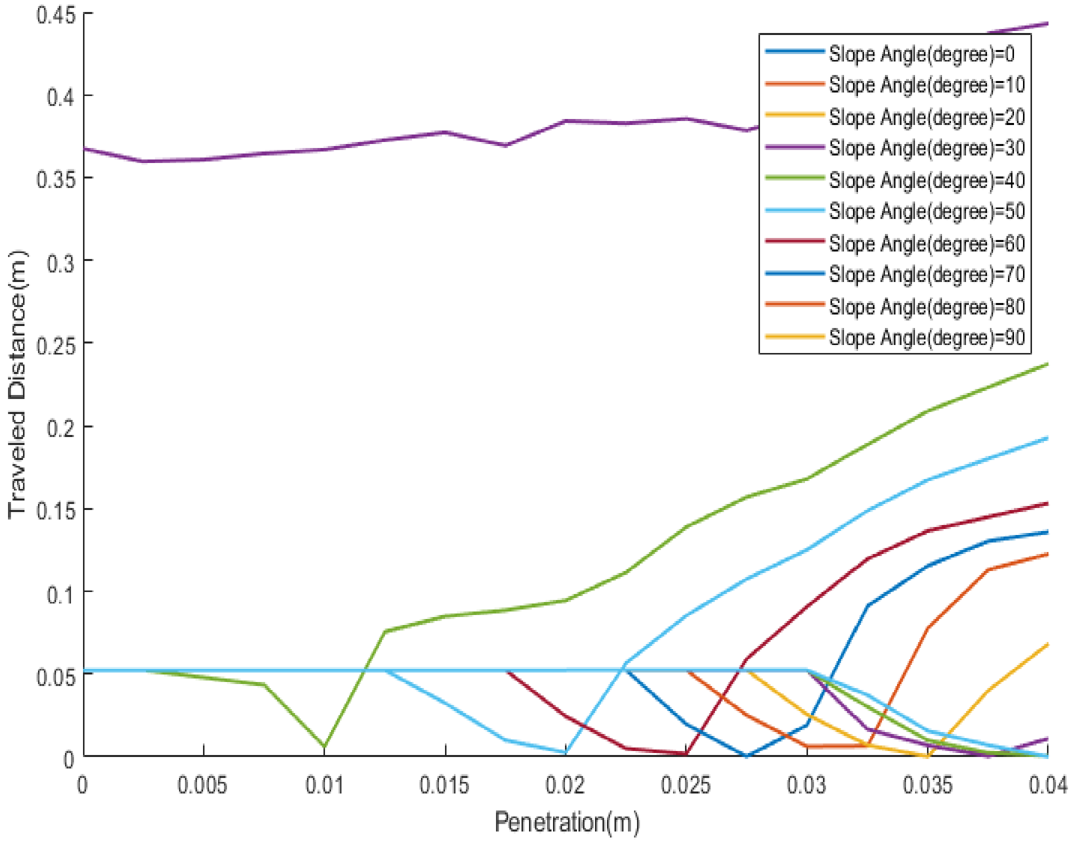

Figure 15 Traveled distance for different slopes and penetrations (2D) (Slope Angle From 0º to 90º)

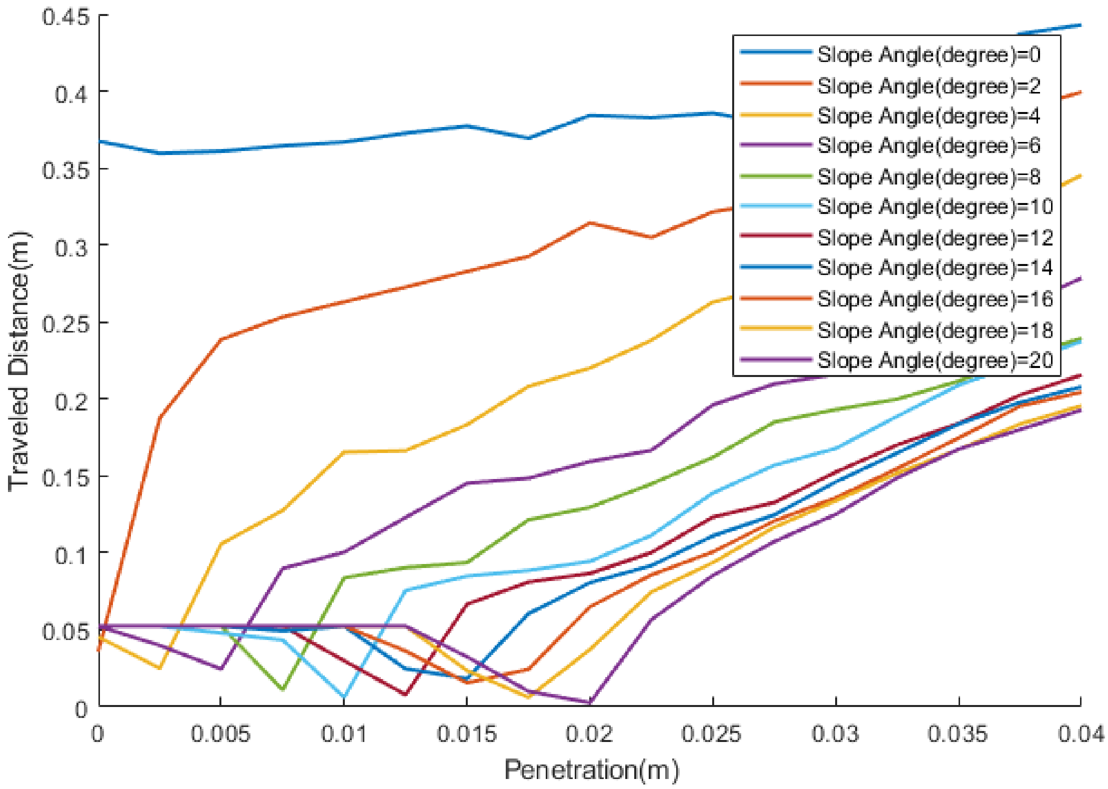

Figure 16 Traveled distance for different slopes and penetrations (2D) (Slope Angle From 0º to 20º)

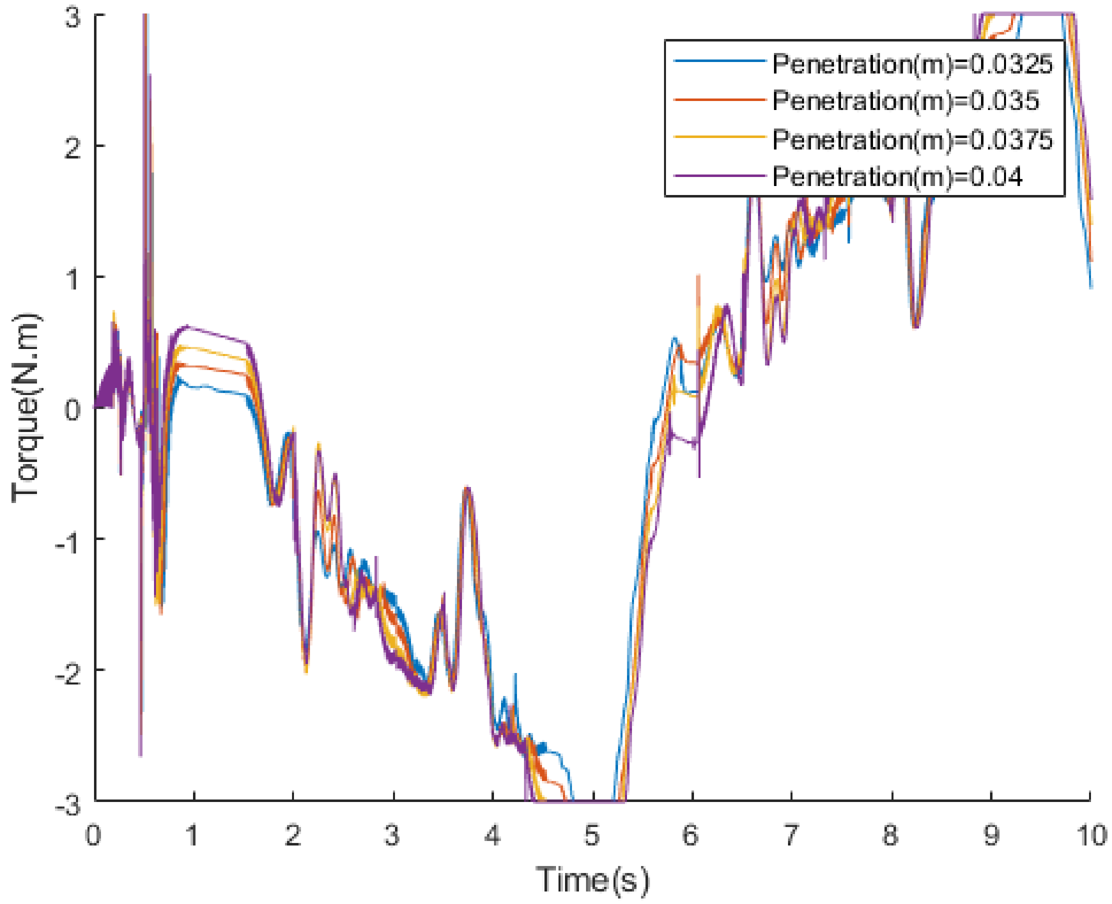

Figure 17 Generated torque for slope angle(degree)=10 in four different penetrations

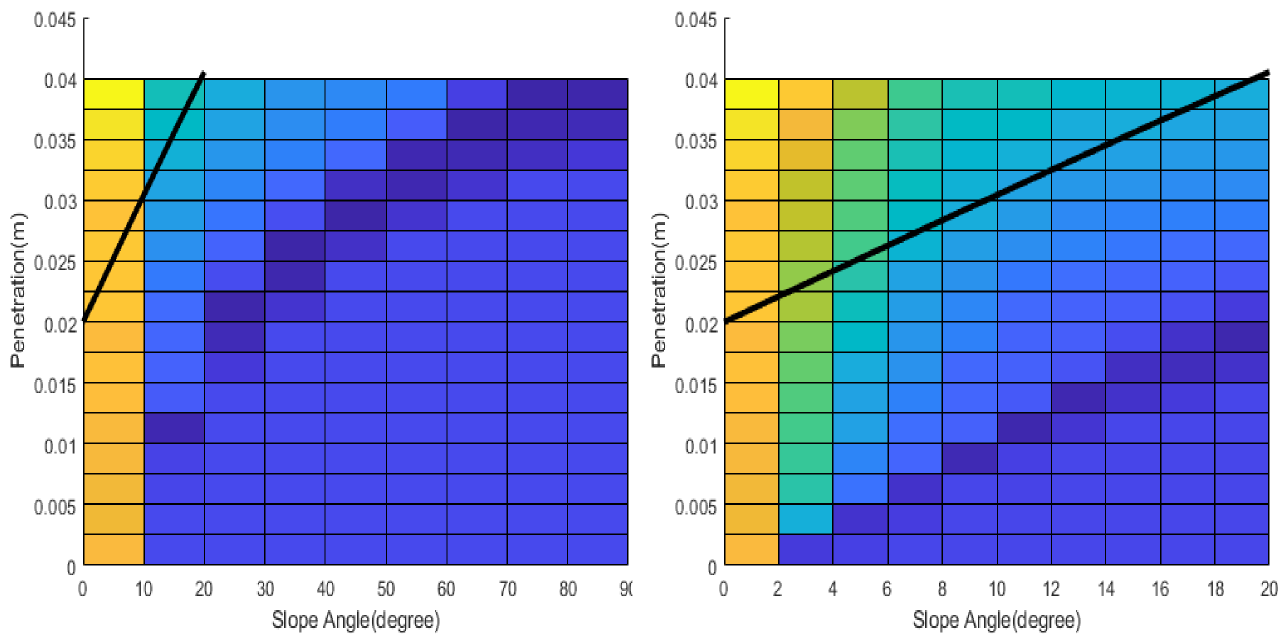

Figure 18 Proposed function for calculating optimal penetration compared with actual results (The yellower the block, the higher travelled distance)

5 Conclusion

This research examines a unique snake robot that moves using a trapezium-like traveling wave. The study first involves calculating the "Number of Amplitude Links" variable, taking into consideration the module geometry and channel width. The trapezium wave angle is then determined and matrix M which specify the angle of each joint of the robot at any step is generated. The size of the M matrix varies based on the number of modules and geometric properties. Using this matrix, the robot's trajectory is planned. To prevent any violations of geometric boundary conditions, we make use of torque control techniques outlined in section (2.1). The controller generates torque by considering the angle error, its time derivative, and its time integration.

Previous research has focused on investigating the locomotion of this robot in straight pipes and bends. However, the robot's ability to navigate sloped surfaces has not been explored.

In this study, we set out to investigate the robot's locomotion in beveled channels and verified our results against existing experimental data. To accomplish this task, we propose planning a trajectory for a wider channel, using a channel width of "D+Dpenetration" instead of just "D". We demonstrated that this adjustment in trajectory planning leads to an increased angular error between the desired trajectory and the actual angles of the robot's joints. This is because, with a channel width of "D", the robot cannot accurately position itself along a trajectory designed for "D+Dpenetration". Considering that the generated torque in actuators is calculated based on the angular error, the torque will increase accordingly. The joints are unable to reach the desired angle from the trajectory due to the limited width of the channel. As a result, when each joint completes its motion step, there is still a non-zero angular error present. This error causes the actuators to push the robot towards the channel walls, resulting in increased normal force and friction between the robot and the walls. This friction helps prevent the robot from slipping on bevel surfaces.

Our analysis has revealed that an increase in Dpenetration can lead to a higher torque requirement. In certain cases, a greater Dpenetration can even cause the generated torque to increase by up to 290%. To determine the optimal value for Dpenetration, we conducted multiple simulations and compared the results. This allowed us to identify the appropriate value for each slope.

Based on these findings, we propose a function that can accurately calculate the optimal value for Dpenetration.

References

[1] S. Hirose, "Biologically Inspired Robots," *Snake-like Locomotors and Manipulators*, 1993, https://lccn.loc.gov/92034986.

[2] A. Crespi, A. Badertscher, A. Guignard, and A. J. Ijspeert, "Swimming and Crawling with an Amphibious Snake Robot," in *Proceedings of the 2005 IEEE International Conference on Robotics and Automation*, 2005: IEEE, pp. 3024-3028, https://doi.org/10.1109/ROBOT.2005.1570574.

[3] S. A. Fjerdingen, P. Liljebäck, and A. A. Transeth, "A Snake-like Robot for Internal Inspection of Complex Pipe Structures (PIKo)," in *2009 IEEE/RSJ International Conference on Intelligent Robots and Systems*, 2009: IEEE, pp. 5665-5671, https://doi.org/10.1109/IROS.2009.5354751.

[4] B. Murugendran, A. A. Transeth, and S. A. Fjerdingen, "Modeling and Path-following for a Snake Robot with Active Wheels," In *2009 IEEE/RSJ International Conference on Intelligent Robots and Systems*, 2009: IEEE, pp. 3643-3650, https://doi.org/10.1109/IROS.2009.5353886.

[5] K. Mateja and W. Panfil, "Design of a Motion System for 3D Printed Snakebot," *Technical Sciences*, Vol. 24, pp. 57–66-57–66, 2021, https://doi.org/10.31648/ts.6820.

[6] T. Lipták, I. Virgala, P. Frankovský, P. Šarga, A. Gmiterko, and L. Baločková, "A Geometric Approach to Modeling of Four-and Five-link Planar Snake-like Robot," *International Journal of Advanced Robotic Systems*, Vol. 13, No. 5, p. 1729881416663714, 2016, https://doi.org/10.1177/1729881416663714.

[7] T. Lipták *et al.*, "Modeling and Control of Two-link Snake," *International Journal of Advanced Robotic Systems*, Vol. 15, No. 2, p. 1729881418760638, 2018, https://doi.org/10.1177/1729881418760638.

[8] T. Dear, B. Buchanan, R. Abrajan-Guerrero, S. D. Kelly, M. Travers, and H. Choset, "Locomotion of a Multi-link Non-holonomic Snake Robot with Passive Joints," *The International Journal of Robotics Research*, Vol. 39, No. 5, pp. 598-616, 2020, https://doi.org/10.1177/0278364919898503.

[9] L. Chen, S. Ma, Y. Wang, B. Li, and D. Duan, "Design and Modelling of a Snake Robot in Traveling Wave Locomotion," *Mechanism and Machine Theory*, Vol. 42, No. 12, pp. 1632-1642, 2007, https://doi.org/10.1016/j.mechmachtheory.2006.12.003.

[10] E. Prada *et al.*, "New Approach of Fixation Possibilities Investigation for Snake Robot in the Pipe," In *2015 IEEE International Conference on Mechatronics and Automation (ICMA)*, 2015: IEEE, pp. 1204-1210, https://doi.org/10.1109/ICMA.2015.7237657.

[11] I. Virgala *et al.*, "Investigation of Snake Robot Locomotion Possibilities in a Pipe," *Symmetry*, Vol. 12, No. 6, p. 939, 2020, https://doi.org/10.3390/sym12060939.

[12] M. J. Koopaee, S. Bal, C. Pretty, and X. Chen, "Design and Development of a Wheel-less Snake Robot with Active Stiffness Control for Adaptive Pedal Wave Locomotion," *Journal of Bionic Engineering*, Vol. 16, pp. 593-607, 2019, https://doi.org/10.1007/s42235-019-0048-x.

[13] A. Selvarajan, A. Kumar, D. Sethu, and M. A. bin Ramlan, "Design and Development of a Snake-robot for Pipeline Inspection," in *2019 IEEE Student Conference on Research and Development (SCOReD)*, 2019: IEEE, pp. 237-242, https://doi.org/10.1109/SCORED.2019.8896254.

[14] A. H. Chang and P. A. Vela, "Shape-centric Modeling for Control of Traveling Wave Rectilinear Locomotion on Snake-like Robots," *Robotics and Autonomous Systems*, Vol. 124, p. 103406, 2020, https://doi.org/10.1016/j.robot.2019.103406.

[15] I. Virgala *et al.*, "A Snake Robot for Locomotion in a Pipe using Trapezium-like Travelling Wave," *Mechanism and Machine Theory*, Vol. 158, p. 104221, 2021, https://doi.org/10.1016/j.mechmachtheory.2020.104221.

[16] H. M. Kim *et al.*, "An In-pipe Robot with Multi-axial Differential Gear Mechanism," In *2013 IEEE/RSJ International Conference on Intelligent Robots and Systems*, 2013: IEEE, pp. 252-257, https://doi.org/10.1109/IROS.2013.6696361.

[17] S. Wakimoto, J. Nakajima, M. Takata, T. Kanda, and K. Suzumori, "A Micro Snake-like Robot for Small Pipe Inspection," In *MHS2003. Proceedings of 2003 International Symposium on Micromechatronics and Human Science (IEEE Cat. No. 03TH8717)*, 2003: IEEE, pp. 303-308, https://doi.org/10.1109/MHS.2003.1249959.

[18] H. Shin, K.-M. Jeong, and J.-J. Kwon, "Development of a Snake Robot Moving in a Small Diameter Pipe," In *ICCAS 2010*, 2010: IEEE, pp. 1826-1829, https://doi.org/10.1109/ICCAS.2010.5669881.

[19] J. Whitman, N. Zevallos, M. Travers, and H. Choset, "Snake Robot Urban Search after the 2017 Mexico City Earthquake," In *2018 IEEE International Symposium on Safety, Security, and Rescue Robotics (SSRR)*, 2018: IEEE, pp. 1-6, https://doi.org/10.1109/SSRR.2018.8468633.

[20] F. Trebuňa, I. Virgala, M. Pástor, T. Lipták, and Ľ. Miková, "An Inspection of Pipe by Snake Robot," *International Journal of Advanced Robotic Systems*, Vol. 13, No. 5, p. 1729881416663668, 2016, https://doi.org/10.1177/1729881416663668.